COBEM 99
XV Congresso Brasileiro de Engenharia Mecânica
15th Brazilian Congress of Mechanical Engineering
22 - 26 de Novembro de 1999 / November 22 - 26, 1999 Águas de Lindóia, São Paulo,

ALTERATION OF THE MODEL DESCRIBING THE STABILIZED HYSTERESIS LOOP

Hani. H. A. El-Sharawy
Jaime T. P. de Castro
Catholic University of Rio de Janeiro, Mechanical Engineering Department
Rua Marquês de São Vicente, 225, Gávea, CEP:22453-900, Rio de Janeiro, RJ, Brazil

Abstract. *The equation describing the stabilized hysteresis loop is based on the Ramberg-Osgood relation for the cyclic stress-strain curve, and employs the same coefficients n′ and K′. This model implies that the expanded cyclic curve should coincide with the shape of the hysteresis loops. It is shown that an acceptable fit is not necessarily observed. A structural and an oil drill tube steels were loaded under alternating strain control. Strain ranged up to 1.8 %. An estimate of the loop shape based on one value of the exponent n′ is not feasible. A better fit is obtained based on two values of the cyclic exponent. The results strongly suggests the dependence of the dynamic strain hardening mechanism on the deformation range. Optimum curve fitting requires adjustment of the model equation.*

Keywords: *Hysteresis loops, modeling, cyclic strain hardening*

1. INTRODUCTION

The cyclic characteristics of metallic materials are determined after alternating strain control fatigue tests. In practice, a power relation is used to describe the stress-plastic strain cyclic relation:

$$\sigma_a = K'(\varepsilon_{ap})^{n'}. \qquad (1)$$

The cyclic strain hardening exponent, n', and coefficient, K', are determined by linear adjustment of the logarithmic form of "Eq. (1)", and are considered to be material constants. "Equation (1)" implies that the amplitudes of a given coordinate (σ_a , ε_{ap}) along the cyclic stress-strain curve are determined at the peak of the corresponding stabilized hysteresis loop. To that effect, the determination of material constants assumes that the material is effectively cyclically stable, the transient material reaction extending up to at most 10% of the crack initiation period.

As for monotonic loading, the Ramberg-Osgood model is used to describe the cyclic stress-strain curve. Independent of the total applied strain range, the model divides the strain amplitude, for a given *stabilized* hysteresis loop, into an elastic and plastic components:

$$\varepsilon_a = \sigma_a / E + (\sigma_a / K')^{1/n'} . \qquad (2)$$

"Equation (2)" describes the stabilized cyclic stress-strain curve. That is, each point on the curve represents a given total strain range and the maximum stress of the corresponding hysteresis loop. The strain and stress amplitudes may be given in terms of the respective ranges, Δ, and "Eq. (2)" becomes:

$$\Delta\varepsilon/2 = \Delta\sigma/2E + (\Delta\sigma/2K')^{1/n'}, \text{ or}$$

$$\Delta\varepsilon = \Delta\sigma/E + 2(\Delta\sigma/2K')^{1/n'} . \qquad (3)$$

The strain and stress ranges in "Eq. (3)" represent the difference between the maximum and minimum strain and stress values for a given strain range and, therefore, describes ½ of the loop cycle. The equation is effectively an expanded form (a scale factor of 2) of the cyclic stress-strain curve, "Eq. (2)". In order to justify the scale factor observation and the validity of "Eq. (3)" as the equation describing the Hysteresis loop shape we analyze the multistage spring-slider model of the cyclic stress-strain curve as shown in "Fig (1)" (Dowling, 1993). the characteristics of the model are observed first on loading, then on unloading.

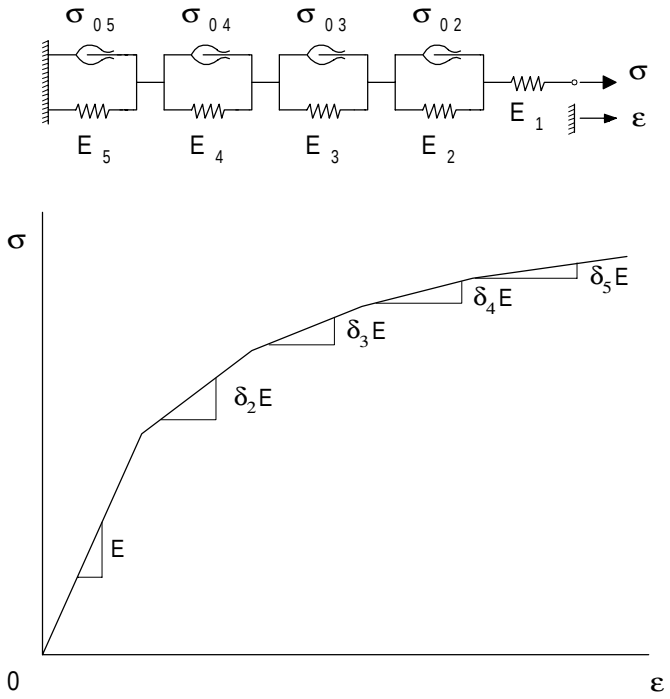

Figure 1- Multistage spring and slider model

1.1. Model analysis on loading

"Figure (1)" shows that the non-linear plastic region may be approximated by a sequence of linear segments of consecutively lower slopes. The number of segments will depend on the sought level of curve adjustment. Each linear segment is modeled by a spring-frictionless slider element. Since the plastic curve tends to level off as the strain (ε) increases, the slope of the consecutive segments decreases, and may be given as a fraction ($\delta_i E$) of the elastic modulus E, where δ_i is the slope-reduction-factor, i = 1,2,3, ..., and $\delta_{i+1} < \delta_i$.

As the material is loaded in tension, the first (independent) spring, E_1, resists the load *alone* up to the yield limit of the first slider, σ_{02}; the limit at which the material is about to flow plastically. Being frictionless, the slider moves under a constant load σ_{02}. Therefore, the load increase above σ_{02} will be supported *only* by the parallel spring, E_2, up to the yield limit of the second slider, σ_{03}. The second spring-slider element will then repeat the sequence of slider-spring movements, and so on. It should be clear that the slider in a given spring-slider element will not move before the applied load attains its yield limit and, due to the parallel connection, the accompanying spring remains stationary while the slider is not moving.

The stress after yielding in a given i stage is given by :

$$\sigma = \sigma_{oi} + E_i \varepsilon_i , \qquad (4)$$

where ε_i is the strain of the corresponding spring. Solving for strain :

$$\varepsilon_i = \frac{\sigma - \sigma_{oi}}{E_i} , \qquad (5)$$

and the total strain after yielding of j stages :

$$\varepsilon = \frac{\sigma}{E_1} + \frac{\sigma - \sigma_{o2}}{E_2} + \frac{\sigma - \sigma_{o3}}{E_3} + \frac{\sigma - \sigma_{o4}}{E_4} + --+ \frac{\sigma - \sigma_{oj}}{E_j} \qquad (6)$$

Since a given spring-slider element will not move before all the previous elements have moved and the slider characteristic yield load is attained, the slope of any linear segment, say $\delta_j E$, will be associated to the stiffness of all springs in series for which the corresponding sliders have yielded. It can be easily shown (Dowling, 1993) that:

$$\delta_j E = \frac{1}{\frac{1}{E_1} + \frac{1}{E_2} + \frac{1}{E_3} + ... + \frac{1}{E_j}} . \qquad (7)$$

1.2. Model analysis during unloading

We consider any stage (say the i^{th} line-segment) of the multistage model of "Fig. (1)". After yielding of that stage, the stress at a given stress-strain point (ε', σ') on the stress-strain curve is given by:

$$\sigma' = \sigma_{oi} + E_i \varepsilon_i' , \qquad (8)$$

where E_i is the slope and ε_i' the strain of the i^{th} line-segment only. It should be understood that $E_i \varepsilon_i'$ is the stress increment sustained in i^{th} stage by the spring only. If the direction of loading is reversed at the point (ε', σ'), the strain ε_i' will not be changed (reduced) before the slider moves (yields) in compression. That is, before the slider stress reaches $-\sigma_{oi}$, neither

the slider nor the spring will move and the stress sustained by the spring, $E_i \varepsilon_i'$, remains unchanged. Therefore, the i^{th} stage remains *locked* during unloading until the resistance of the slider is again overcome at a slider stress of $-\sigma_{oi}$. Accordingly, the stress, on the strain-stress curve, at the point of reversed yielding of the i^{th} stage is given by :

$$\sigma'' = -\sigma_{oi} + E_i \varepsilon_i' \ , \qquad (9)$$

and the stress difference, $\Delta\sigma''$, between the point of stress reversal (ε', σ') and the point of reversed yielding of the i^{th} stage, is the difference between "Eq. (8)" – "Eq. (9)" :

$$\Delta\sigma'' = \sigma' - \sigma'' = 2\sigma_{oi} \ . \qquad (10)$$

"Equation (10)" shows that, based on a multistage slider-spring element, the stress difference, $\Delta\sigma''$, leading to the reversed yielding of a given stage is twice the stress required for moving the same slider in monotonic tension. Beyond the point of reversed yielding of the i^{th} stage, the stress on the slider remains at $-\sigma_{oi}$, and the further increase in the stress difference, $\Delta\sigma - 2\sigma_{oi}$ is taken up by the elastic *negative* deflection of the associated spring only. Therefore, the contribution of the the i^{th} stage on the strain change is :

$$\Delta\varepsilon_i = \frac{\Delta\sigma - 2\sigma_{oi}}{E_i}, \qquad (11)$$

and the total strain change is the sum of all yielded stages :

$$\Delta\varepsilon = \frac{\Delta\sigma}{E_1} + \frac{\Delta\sigma - 2\sigma_{o2}}{E_2} + \frac{\Delta\sigma - 2\sigma_{o3}}{E_3} + \text{----} + \frac{\Delta\sigma - 2\sigma_{oj}}{E_j}, \qquad (12)$$

where all the stages through the j th stage have reverse yielded. Recalling that the point of load reversal is (ε', σ'), the new coordinate on the (σ , ε) axis after reverse yielding of a given number of stages is given by :

$$\sigma = \sigma' - \Delta\sigma \ , \qquad \varepsilon = \varepsilon' - \Delta\varepsilon \ . \qquad (13)$$

The slope, $\frac{\partial\sigma}{\partial\varepsilon}$, at any point of the stress-strain path during reverse loading may be calculated by considering "Eq. (12)" and "Eq. (13)" :

$$\frac{\partial\sigma}{\partial\varepsilon} = \frac{1}{\frac{1}{E_1} + \frac{1}{E_2} + \frac{1}{E_3} + \ldots + \frac{1}{E_j}}, \qquad (14)$$

"Equation (14)" and "Eq. (7)" show that the slope of a given stage on reverse loading is the *same* as the slope of the very stage on monotonic loading. At the same time, "Eq. (10)" show that the stress difference of a given slider on reversed yielding is twice the monotonic yield stress. In other words, the intervals between reversed yielding are twice as large as the

intervals between the corresponding monotonic yielding intervals. This shows that, during reverse loading, the curve of the strain-stress path has the same shape as monotonic loading, but is expanded by a scale factor of two and, consequently, the length of the straight-line segments of the unloading path is double that of the corresponding monotonic segments

The monotonic strain response, "Eq. (6)" and the strain response during unloading, "Eq. (12)", may be written as a function of the stress and stress difference, respectively:

$$\varepsilon = \frac{\sigma}{E_1} + f(\sigma) \qquad (15)$$

$$\frac{\Delta\varepsilon}{2} = \frac{\Delta\sigma}{2E_1} + f\left(\frac{\Delta\sigma}{2}\right), \quad \text{or}$$

$$\Delta\varepsilon = \frac{\Delta\sigma}{E_1} + 2f\left(\frac{\Delta\sigma}{2}\right). \qquad (16)$$

Since the stress and strain increments are always referred to the reversal point, "Eq. (16)" will lead to "Eq. (3)" when the end point on the reversed stress-strain curve is another reversal point.

1.3. Loop shape

As shown above, "Eq. (16)" defines the stress-strain path up to $1/2$ the fatigue loading cycle. Therefore, the loop shape is determined by solving "Eq. (3)" twice; once for positive and another for negative increments of strain. The positive increments curve is referenced to the minimum strain value, and the negative increments curve is referenced to the maximum strain value.

Given that the area of the hysteresis loop is a measure of the plastic work expended per cycle, an accurate description of the loop form is necessary in order to evaluate the material capacity to accommodate cyclic plasticity. It is noted that the incremental form of the Ramberg-Osgood model, "Eq. (3)", defines the loop shape in terms of the material cyclic constants. This paper analyzes the validity of the extended Ramberg-Osgood model and suggests necessarily adjustments.

2. MATERIAL AND EXPERIMENT

Cylindrical 1020 and API X-70 steels specimens were fatigued under alternating strain control. Samples dimension was optimized to prevent buckling. Both steels were machined to a gauge length of 15 mm, a specimen cross section of 7.5 mm for the API X-70 steel and 13 mm for the 1020 steel. The applied strain ranges are shown in Table 1. Amplitude ranges above 1.20 % were not feasible in the API X-70 Steel due to specimen bucking.

Table 1- Applied Strain Amplitude %

1020 steel	0.25	0.40	0.60	0.80	1.00	1.20	1.40	1.60	1.80
API X-70	0.40	0.60	0.70	0.80	0.90	1.00	1.20		

Data acquisition was programmed to permit a sufficiently continuous record of the sample load reaction. The record permits the identification of the transient, cyclic stability and the crack propagation periods. Minimum alterations of hysteresis loop shape may thus be

identified. The stability region was identified, or assumed were necessary, after the plot of the variation of the maximum and minimum load. The cyclic stress-strain curve was determined for each steel by adjusting the peaks of the concentric loops.

The theoretical hysteresis loops were determined by substituting into the incremental model as explained above. The level of discrepancy between the model and the experimental loops was determined by superimposing the respective experimental and theoretical curves.

3. RESULTS AND DISCUSSION

"Figure (1)" shows the typical cyclic behavior of the 1020 steel. The steel load reaction stabilizes after a given softening period. The relative transient period, given as the ratio of (transient period / stability period), is in the range of 30-40 % as shown in Table 2, which is well above the generally accepted 10 % period. This difference may not be attributed to a material strain rate sensitivity given that the test frequency was varied between 0.2 to 5 Hz. Also, the difference may not be attributed to sample misalignment since both the maximum and minimum loads typically converge to stability at the same rate, as shown in "Fig. (1)".

Table 2- Relative Transient Period

1020	Strain Amp. %	0.25	0.40	0.60	0.80	1.00	1.20	1.40	1.60	1.80
Steel	Transience %	0.39	0.40	0.33	0.40	0.31	0.38	0.34	0.40	0.29
X-70	Strain Amp. %	0.40	0.60	0.80	0.70	0.90	1.00	1.20		
Steel	Transience %	0.41	0.40	0.40	0.39	0.36	0.40	0.35		

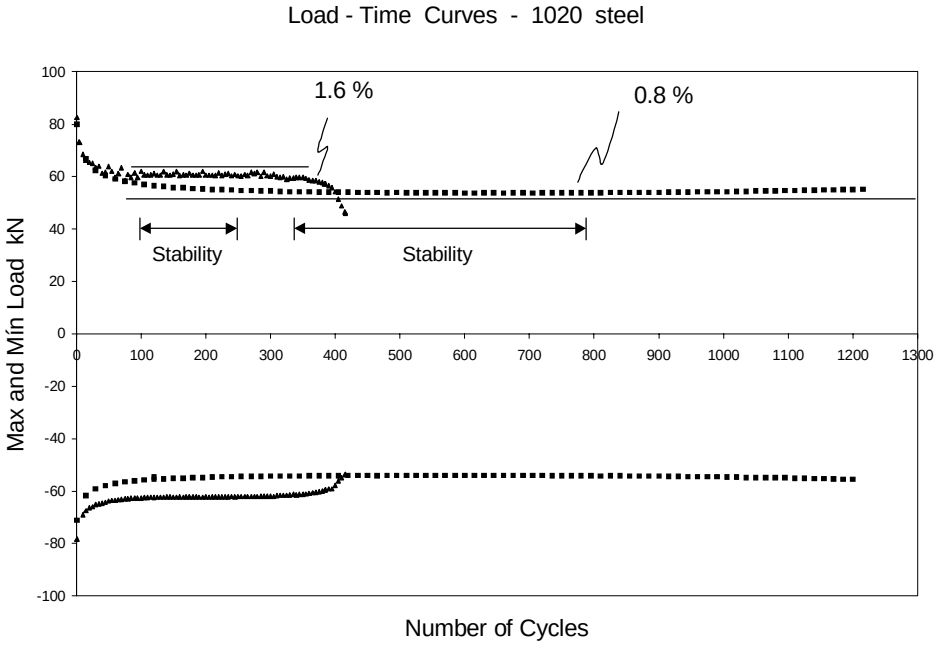

Figure 1- Cyclic stability in 1020 steel

On the other hand, "Fig. (2)" shows that cyclic softening is continuous in the API X-70 steel. In this case, relative stability was taken as the range of constant (linear) softening rate. This procedure permits the identification of a 'stabilized' loop representative of the steel behavior at the given strain range, namely the mid range loop. Table 2 shows that, as for the 1020 steel, relative stability is, in general, independent of the strain amplitude.

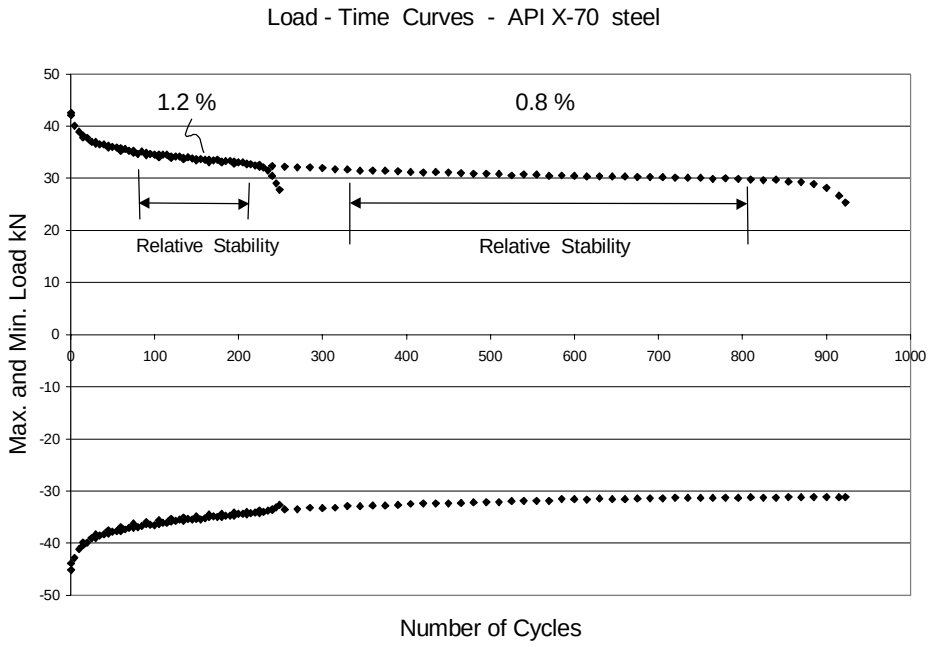

Figure 2- Relative Cyclic stability in API X-70 steel

"Figures (3) and "Fig. (4)" show the cyclic stress-strain curves superposed on the respective stabilized hysteresis loops. In order to guarantee coherent comparison with the monotonic behavior, the cyclic constants n′ and K′ were determined by considering *only* the peak loads of the hysteresis loops. It should be mentioned that adjustment of a cyclic stress-strain curve using the compressive peaks of the stabilized loops returns slightly higher values of the cyclic strain hardening exponent, n′, (El-Sharawy & Castro, 1998). As expected, the 1020 steel show, an exponential work hardening cyclic behavior, while "Fig. (4)". shows the cyclic behavior of the API steel nears an elastic-perfectly plastic material.

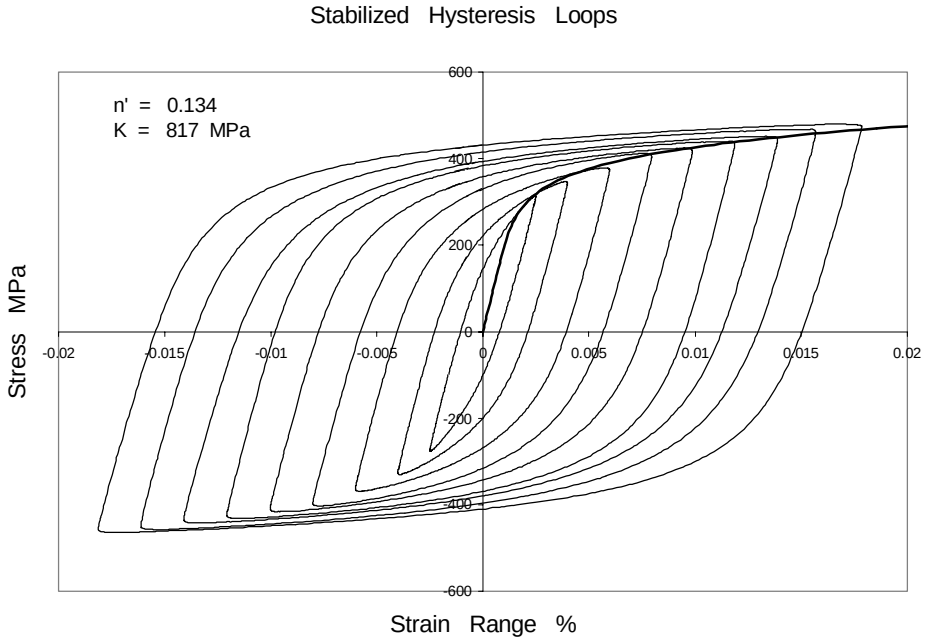

Figure 3 Stabilized Hysteresis Loops and Cyclic Stress-Strain Curve - 1020 Steel

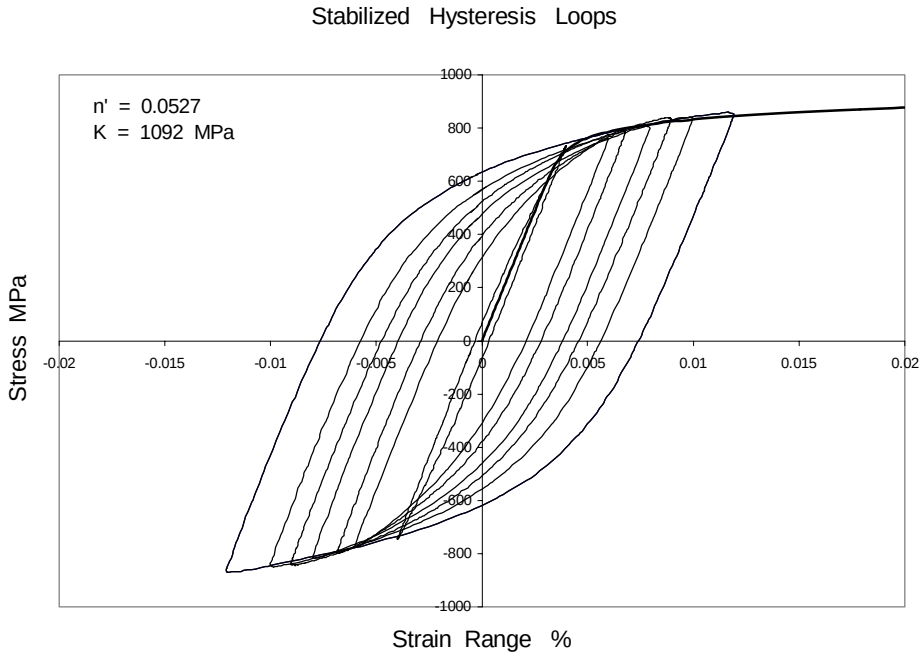

Figure 4 Stabilized Hysteresis Loops and Cyclic Stress-Strain Curve - API X-70

3.1 Model and experimentally determined loops

Changing material characteristics are generally considered at the two ends of fatigue crack initiation. Shang and Ding (1996) studied the transient behavior in aluminum and steel alloys by defining a changing cyclic softening factor. At the other end, Abel (1997) analyzed the loop shape in order to understand the process of plastic instability.

Variations of the cyclic strain hardening exponent are usually related to the transient period (Berkovits, 1987). The parameter is expected to remain constant within the stability region and little attention has been given to possible variation during this period. However, as shown in “Fig. (5)”, the model may deviate significant from the experimental curve.

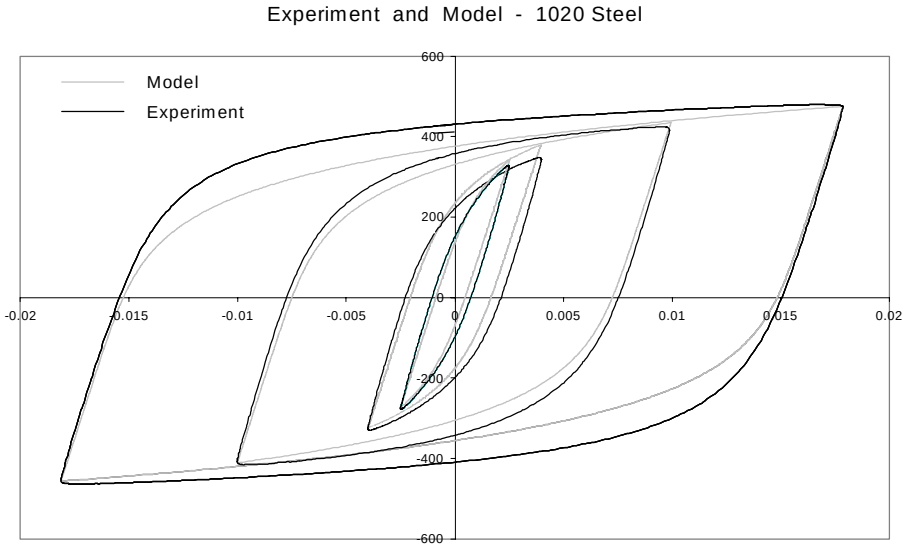

Figure 5 Model and experimental curves (one cyclic strain hardening exponent)

"Figure (5)" shows clearly that the discrepancy increases as the strain range is increased, the discrepancy is pronounced at the beginning of the plastic range and is gradually reduced until both curves coincide at the other load reverse point. This behavior is also observed in the API steel. The deviation of the model from the experimental curve is attributed to the limitation of the spring and slider rheological model of "Fig. (1)". If, on the one hand, the model provides a useful idealization of cyclic loading, it does not include time-dependent effects or show other complexities observed in real materials (Dowling, 1993).

Besides, the model of "Eq. (1)" follows the monotonic approach and relates the stress to the plastic strain through *one* strain hardening exponent. This approximation is essentially valid for medium carbon steel materials. However deviations from a one exponent relationship are frequently observed, where the experimental stress-plastic strain points are better described by two straight lines on the log-log plot of the monotonic model (Dieter, 1976).

In order to investigate the effect of a variable strain hardening coefficient, the strain range was divided into two regions and the exponent recalculated for each region. The first region extended up to 0.6 %, and as shown in "Fig. (6)" a much better fit is obtained.

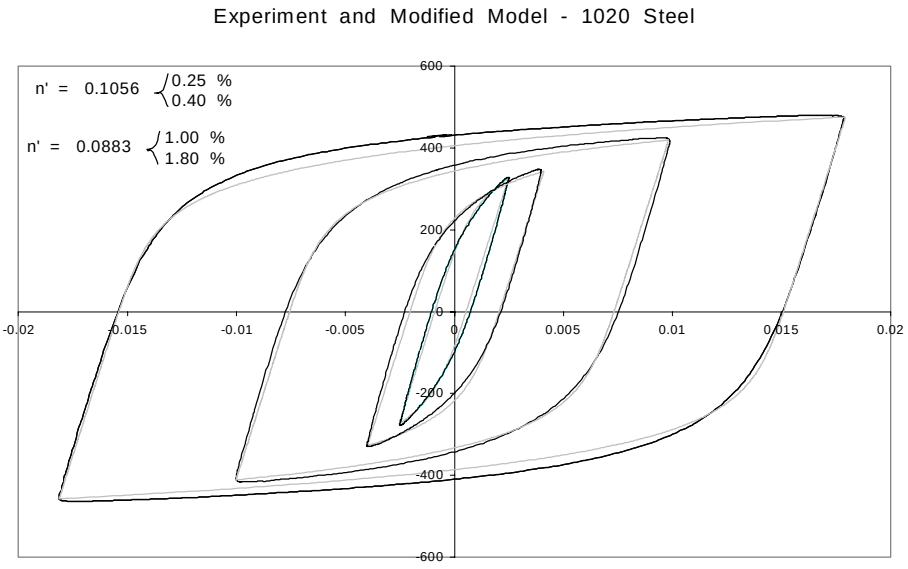

Figure 6 Model and experimental curves (two cyclic strain hardening exponent)

Though the discrepancy is considerably reduced by adopting two strain hardening exponent, the model continues to deviate from experiment at higher strain ranges. The deviation of experiment from model may not be attributed to specimen buckling since the discrepancy is symmetrical about the stress axis. It may be suggested that coincidence of model and experiment at higher strain ranges (1.00 and 1.80 %) can be achieved by substituting an even lower n′ value. However, this will push the start of the plastic strain range (end of the elastic straight line range) up to higher, unrealistic, stresses. Also, the difference between constant frequency and constant stain rate responses should be investigated. In this paper, fatigue testing was performed under constant frequency. This means that the strain rate was increased with the increase in the applied strain range; that is possible inelastic effects on the stress-strain response were different at each strain range.

It may be concluded that two strain hardening exponents permit a much better fit of the stabilized hysteresis loops. However, refinement is still required. To this end, work is in progress to introduce alterations in the expanded form of the Ramberg-Osgood model.

ACKNOWLEDGEMENT

The authors would like to thank the CENPES research center for supplying the API steel tube material

REFERENCES

(1) Abel, A., Plastic instabilities during fatigue cycling, Proceedings of the Ninth International Conference on Fracture (ICF 9), April 1-5, Sydney, vol. 3, 1997, pp. 1251-1259.

(2) Berkovits, A., 1987, Variation of the cyclic strain-hardening exponent in advanced Aluminum Alloys, International Journal of Fatigue, Vol. 9, No. 4, pp. 229-232.

(3) Dieter, G. E., 1976, Mechanical Metallurgy, McGraw Hill, Tokyo

(4) Dowlling, N. E., 1993, Mechanical Behavior of Metals: Engineering Methods for Deformation, Fracture, And Fatigue, Prentice-Hall, New Jersey.

(5) El-Sharawy, H. H. A. & Castro, J. T. P., 1998, Comparison of the coefficients n′ e K′ of the cyclic stress-strain curve in tension and compression, Proceedings of the 13th Brazilian Congress of Engineering and Material Science (CBECIAMT), December 6-9, Cuirtiba, pp. 1153-1157

(6) Shang, H., and Ding, H., 1996, Low cycle fatigue stress-strain relation: model of cyclic hardening or cyclic softening materials, Engineering Fracture Mechanics, Vol. 54, No. 1, pp. 1-9.